




## Article

# Simultaneous Removal of Pb<sup>2+</sup> and Zn<sup>2+</sup> Heavy Metals Using Fly Ash Na-X Zeolite and Its Carbon Na-X(C) Composite

Rafał Panek <sup>1,\*</sup>, Magdalena Medykowska <sup>2,\*</sup>, Małgorzata Wiśniewska <sup>2</sup>, Katarzyna Szewczuk-Karpisz <sup>3</sup>, Katarzyna Jędruchniewicz <sup>2</sup> and Małgorzata Franus <sup>1</sup>

<sup>1</sup> Faculty of Civil Engineering and Architecture, Lublin University of Technology, Nadbystrzycka 40, 20-618 Lublin, Poland; m.franus@pollub.pl

<sup>2</sup> Department of Radiochemistry and Environmental Chemistry, Institute of Chemical Sciences, Faculty of Chemistry, Maria Curie-Skłodowska University in Lublin, M. Curie-Skłodowska Sq. 3, 20-031 Lublin, Poland; wisniewska@hektor.umcs.lublin.pl (M.W.); k.jedruchniewicz@poczta.umcs.lublin.pl (K.J.)

<sup>3</sup> Institute of Agrophysics, Polish Academy of Sciences, Doświadczalna 4, 20-290 Lublin, Poland; k.szewczuk-karpisz@ipan.lublin.pl

\* Correspondence: r.panek@pollub.pl (R.P.); m.medykowska@poczta.umcs.lublin.pl (M.M.)

**Abstract:** Pure zeolite (Na-X) and a zeolite–carbon composite (Na-X(C)) were investigated as adsorbents of heavy metals—Pb<sup>2+</sup> and Zn<sup>2+</sup> from an aqueous solution. These materials were synthesized from fly ash—a waste from conventional hard coal combustion. Both solids were characterized using XRD, SEM-EDS, nitrogen adsorption/desorption, particle size and elemental composition analyses. The adsorption study was performed at pH 5 in the systems containing one or two adsorbates simultaneously. The obtained results showed that the pure zeolite was characterized by a more developed surface area (728 m<sup>2</sup>/g) than its carbon composite (272 m<sup>2</sup>/g), and the mean pore diameters were equal to 1.73 and 2.56 nm, respectively. The pure Na-X zeolite showed better adsorption properties towards heavy metals than its Na-X(C) composite, and Zn<sup>2+</sup> adsorbed amounts were significantly higher than the Pb<sup>2+</sup> ones (the highest experimental adsorption levels were: for Zn<sup>2+</sup>—656 and 600 mg/g, and for Pb<sup>2+</sup>—575 and 314 mg/g, on the Na-X and Na-X(C) surfaces, respectively). The zinc ions are exchanged with the cations inside the zeolite materials structure more effectively than lead ions with a considerably larger size. In the mixed systems, the competition between both heavy metals for access to the active sites on the adsorbent surface leads to the noticeable reduction in their adsorbed amounts. Moreover, the hydrochloric acid was a better desorbing agent for both heavy metals, especially Pb<sup>2+</sup> one (desorption reached 78%), than sodium base (maximal desorption 25%).

**Keywords:** fly ash; synthetic zeolites; zeolite–carbon composites; adsorbents of heavy metals; competitive adsorption; simultaneous removal; adsorption kinetics



**Citation:** Panek, R.; Medykowska, M.; Wiśniewska, M.; Szewczuk-Karpisz, K.; Jędruchniewicz, K.; Franus, M. Simultaneous Removal of Pb<sup>2+</sup> and Zn<sup>2+</sup> Heavy Metals Using Fly Ash Na-X Zeolite and Its Carbon Na-X(C) Composite. *Materials* **2021**, *14*, 2832. <https://doi.org/10.3390/ma14112832>

Academic Editor: Lubomira Tosheva

Received: 16 April 2021

Accepted: 23 May 2021

Published: 25 May 2021

**Publisher's Note:** MDPI stays neutral with regard to jurisdictional claims in published maps and institutional affiliations.



**Copyright:** © 2021 by the authors. Licensee MDPI, Basel, Switzerland. This article is an open access article distributed under the terms and conditions of the Creative Commons Attribution (CC BY) license (<https://creativecommons.org/licenses/by/4.0/>).

## 1. Introduction

Zeolites are hydrated aluminosilicates of metals from the I and II group, formed in hydrothermal processes of rock transformation in the environment or synthesized by chemical methods. These materials are characterized by unique structures. They are composed of silicon and aluminum tetrahedrons, called Primary Building Units (PBU). The tetrahedrons are connected by oxygen atoms, which create larger repeating geometric forms called polyhedrons. They are signed as Secondary Building Units (SBU). As a result of a combination of the units, three-dimensional zeolite structures such as cubes, hexagonal pyramids or cuboctahedrons are formed. Furthermore, the specific distribution of tetrahedrons creates an internal system of channels filled, for example, with water molecules (called zeolite water). Zeolites are extremely diverse in their chemical composition. Usually, the negative charge of the crystal lattice, easy exchange of extra-network cations, homogeneous micropore size and satisfactory thermal and hydrothermal stability are features typical

for the described materials [1,2]. Zeolites exhibit well-developed specific surface, high sorption capacity and high ion exchange [3–6]. Due to this fact, they are called molecular sieves [1]. They can adsorb not only cations, for instance, heavy metal ions, but also organic substances or anions from aqueous solutions. The properties of natural zeolites can be improved by their modification using ion exchange, acid treatment or functionalization with surfactants.

Heavy metals have a negative impact on the natural environment and living organisms. They are often toxic, cancerogenic and can damage the immune and nervous system. Therefore, it is important to monitor and, if possible, remove this type of contamination from water, sewage and soil. Currently, scientists are focusing more and more on the use of sorbents obtained from various types of waste for heavy metals removal. Shahrokhi-Shahraki et al. confirmed that the activated carbon from pulverized waste tire shows a better sorption performance towards  $\text{Pb}^{2+}$ ,  $\text{Cu}^{2+}$  and  $\text{Zn}^{2+}$  than its commercial counterpart [7]. Other sorbents used for the removal of heavy metals are zeolites from the sodalite and gismodite groups obtained from fly ash [8]. Fly ash-derived zeolites have also been used in simultaneous sorption in mixed systems (even five different heavy metals) [9,10]. Similar or even better sorption results were also obtained in another study, in which fly ash-derived zeolites from the faujasite group were used for heavy metals removal ( $\text{Pb}^{2+}$ ,  $\text{Cu}^{2+}$ ,  $\text{Cd}^{2+}$ ,  $\text{Zn}^{2+}$ ,  $\text{Co}^{2+}$ ) in an aqueous solution [11].

In this paper, zeolite (Na-X) and novel zeolite–carbon composite (Na-X(C)) as adsorbents of heavy metal ions are presented. The sorption capacity of the prepared materials relative to two heavy metals,  $\text{Pb}^{2+}$  and  $\text{Zn}^{2+}$ , was investigated. Other scientists have also tested the adsorption abilities of modified and non-modified zeolites relative to the selected metal ions. However, they did not observe spectacularly high adsorption capacities. Kragović et al. [12] investigated natural zeolite (NZA) and zeolite modified via alginate (FRA) and noted that the adsorbed amount on NZA was 102 mg/g and 133 mg/g for FRA. Kim et al. [13] used nanoscale zero-valent iron to obtain the zeolite composite (Z-nZVI) and stated that the  $\text{Pb}^{2+}$  adsorbed amount on this material was equal to 96.2 mg/g. Li et al. [14] also examined zeolite-supported nanoscale zero-valent iron and stated that the adsorption capacity of this material relative to  $\text{Pb}^{2+}$  ions was 85.37 mg/g. Wang et al. [15] investigated the zeolitic imidazolate framework grown on graphene oxide (ZIF-8@GO) and obtained maximum adsorption capacity for  $\text{Pb}^{2+}$  ions equal to 356 mg/g. Abdelrahman et al. [16] used rice husks and aluminum can waste to obtain geopolymer–zeolite products (G3). The adsorbed amount of  $\text{Zn}^{2+}$  ions on this material was 131.93 mg/g. Wang et al. [17] synthesized  $\text{SiO}_2$  encapsulated natural zeolite for the removal of heavy metal ions. The amount of adsorbed  $\text{Pb}^{2+}$  ions on this solid was 186 mg/g, whereas, for  $\text{Zn}^{2+}$  ions, it was 9 mg/g. The zeolite–carbon composites have not been reported yet. Thus, the authors decided to examine precisely these materials.

The adsorbents used in the experiments were manufactured in the process of hydrothermal conversion of high-carbon fly ash (HCFA) [18–20]. This byproduct is accounted for 65–95% of total waste produced in the energy sector. Therefore, both adsorbents were produced from waste in one cycle of the HCFA treatment process—Na-X(C) composite directly from HCFA and Na-X from the secondary waste generated during previous synthesis (silica-rich solution). The whole process was conducted on a semi-technical scale, which can be applied in industries in the near future. Owing to these facts, the solids used in the study have an undoubtedly innovative nature. In order to achieve the full characterization of zeolite and zeolite–carbon composite, various methods, such as SEM-EDS, XRD, nitrogen adsorption/desorption, elemental analysis, potentiometric titration, zeta potential measurement, etc., were applied. The adsorption of heavy metal ions was investigated in the single and mixed systems, i.e., containing one or two heavy metal types at the same time. This allowed for recreating the natural conditions and show the influence of one adsorbate on the adsorption of another one. Contamination in soils by heavy metal ions is a huge environmental problem originating from anthropogenic activities, such as mining, the chemical industry, agriculture or atmospheric deposition. Especially near industrial

bases, there is a strong possibility of dangerous pollution posing a risk to organisms for a long time [21–23]. The performed experiments allowed to state whether selected materials allow for highly effective cleaning of soil and water.

## 2. Materials and Methods

### 2.1. Adsorbent Preparation

In the first stage of the experiment, the zeolite–carbon composite (Na-X(C)) was obtained. The starting material was fly ash from the Janikowo thermal power plant (Janikowo, Poland) produced as a result of conventional hard coal combustion. The carbon–zeolite composite was created in the hydrothermal reaction of fly ash (25 kg) with a 3 M aqueous sodium hydroxide solution (90 L) on the technological line for the synthesis of ash zeolites for 48 h in 80 °C [19]. On the other hand, Na-X was obtained from a waste solution rich in silicon and aluminum (formed during the synthesis of Na-X(C)) according to the procedure contained by Panek et al. [18]. Briefly, this waste solution was mixed with a sodium hydroxide solution containing Al foil and then subjected to a hydrothermal reaction. Mineralogical, structural and textural characteristics were conducted on both sorbents.

### 2.2. Solids Characteristics

Textural parameters were measured on an ASAP 2020 apparatus (Micromeritics Instrument Corporation, Norcross, GA, USA) using low-temperature nitrogen adsorption/desorption isotherms at a liquid nitrogen temperature of  $-194.85$  °C over a range of relative pressures  $p/p_0$  ranging from  $1.5 \times 10^{-7}$  to 0.99. The shape analysis of nitrogen vapor adsorption isotherms was characterized based on the IUPAC classification [24,25]. Samples were degassed twice: (1) at 300 °C for 12 h under reduced pressure, (2) 4 h at 300 °C (prior to analysis). The specific surface area ( $S_{\text{BET}}$ ) of adsorbents was determined using the BET equation. The micropore volume ( $V_{\text{micro}}$ ) and area ( $S_{\text{micro}}$ ) were determined using the ‘t-plot’ method. In turn, the pore size distribution in the adsorbent was calculated using the BJH method.

The elemental composition was determined by semi-quantitative energy dispersive X-ray fluorescence on an Epsilon 3 spectrometer (Panalytical, Eindhoven, The Netherlands). The apparatus was equipped with a Rh 9 W, 50 kV, 1 mA X-ray lamp, a 4096 channel spectrum analyzer and a high-resolution solid-state SDD detector cooled by a Peltier cell. Obtained results included the LOI.

The particle size was investigated based on laser diffraction phenomena on a Mastersizer 3000 instrument (Malvern Panalytical, Malvern, UK). The test was conducted in an aqueous environment in the HYDRO EV attachment. The Mie theory was used during measurements in the measurement range (0.01  $\mu\text{m}$  to 2 mm).

A morphological analysis in the microarray of the studied materials was carried out on a Quanta 250 FEG scanning electron microscope (FEL, Hillsboro, OR, USA) equipped with an EDS attachment from EDAX. The experiments were conducted on samples sprayed with a conductive carbon layer at an accelerating voltage of 15 keV.

The mineral composition of sorbents was determined by X-ray diffraction on X'Pert Pro MPD (Panalytical, Eindhoven, The Netherlands). A copper lamp ( $\text{CuK}\alpha = 1.54178$  Å) was used as the emission source. The test was conducted over an angular range of  $5$ – $65^\circ$   $2\theta$  with a step equal to  $0.02^\circ$   $2\theta$  lasting 5 s. The X'Pert Highscore software was used to process the diffraction data. The identification of mineral phases was based on the PDF-2 release 2010 database formalized by JCPDS-ICDD.

The surface functional groups of zeolite and zeolite–carbon composite were determined using Fourier transform infrared spectroscopy (FTIR spectrometer, Nicolet 8700A, Thermo Scientific, Waltham, MA, USA). The solids were analyzed as pellets with KBr.

### 2.3. Adsorption/Desorption Measurements

The adsorbed amounts of heavy metal ions on the Na-X and Na-X(C) surfaces were determined using the static method, based on the decrease in the adsorbate concentration

in the solution after the adsorption process [26]. The samples (10 cm<sup>3</sup>) were prepared using 0.003 g of the solid, supporting electrolyte (0.001 M NaCl) and heavy metal ion with the concentration in the range of 10–200 ppm. In the mixed systems, the concentration of ions was equal to 100 ppm. The bulk solutions of heavy metal (Pb(NO<sub>3</sub>)<sub>2</sub> and Zn(NO<sub>3</sub>)<sub>2</sub>) had a concentration of 1000 ppm. The appropriate concentration of the adsorbates was obtained by diluting them with demineralized water. The adsorption process was carried out for 3 h, at pH 5, under continuous shaking conditions (100 rpm, Unimax 1010, Heidolph, Schwabach, Germany). The pH value was adjusted in the samples using 0.1 M NaOH or 0.1M HCl and pHmeter Beckman (Pasadena, CA, USA) when adsorbates were present in the suspensions. The used HCl/NaOH volumes were maximum 0.005 cm<sup>3</sup>. After the adsorption completion, the solid was separated by centrifugation (8000 rpm, 310 b, Mechanika Precyzyjna, Poland). The heavy metal ions concentration in the supernatants was determined using inductively coupled plasma-optical emission spectrometry (Thermo Scientific iCAP™ 7200 ICP-OES analyzer, Waltham, MA, USA). The adsorption isotherm data were fitted to the Langmuir (Equation (1)) and Freundlich (Equation (2)) models [26,27]:

$$q_e = \frac{q_m K_L C_e}{1 + K_L C_e} \quad (1)$$

$$q_e = K_F C_e^{1/n} \quad (2)$$

where  $K_F$  and  $K_L$ —the Freundlich (mg/g (mg/dm<sup>3</sup>)<sup>-1/nF</sup>) and Langmuir (dm<sup>3</sup>/mg) parameters,  $q_e$ —the equilibrium adsorption capacity (mg/g),  $C_e$ —the equilibrium liquid phase concentration (mg/L),  $q_m$ —the maximum adsorption capacity in Langmuir model (mg/g),  $n$ —the Freundlich constant related to adsorption intensity.

The samples for kinetics study were prepared using 100 ppm of heavy metal ions, supporting electrolyte (0.001 M NaCl) and 0.003 g of Na-X or Na-X(C). The adsorption was carried out for a specific time (10–200 min), at pH 5, under continuous shaking conditions. After filtration of the samples using paper filters (389, Ahlstrom Munktell, Helsinki, Finland), the concentration of heavy metal ions in the clear solutions was determined using ICP-OES. The paper filters were used to isolate the solid more quickly, which is necessary for correct kinetic measurements. The obtained results were modelled using pseudo-first-order (PFO, Equation (3)) and pseudo-second-order equations (PSO, Equation (4)) [28,29]:

$$\frac{dq_t}{dt} = k_1 (q_e - q_t) \quad (3)$$

$$\frac{dq_t}{dt} = k_2 (q_e - q_t)^2 \quad (4)$$

where  $q_e$ —the adsorbed amount at equilibrium (mg/g),  $q_t$ —the adsorbed amount after time 't' (mg/g),  $k_1$  (1/min) and  $k_2$  (g/mg·min)—the equilibrium rate constants.

Desorption rate was determined using the solids obtained after the adsorption, separated from the samples of initial concentration of heavy metal ions equal to 100 ppm. The solids were transferred to 10 mL of 0.1 M HCl or 0.1 M NaCl solutions and the desorption process was performed for 1 h, under continuous shaking (100 rpm, Unimax 1010, Heidolph, Schwabach, Germany). After that, the separation of the solids from the solutions was repeated and the ion concentration was determined by ICP-OES.

The one result of the adsorbed/desorbed amount was the average of three repetitions. The average error did not exceed 5%.

#### 2.4. Electrokinetic Parameters Determination

The surface charge density ( $\sigma_0$ ) of the zeolite and its carbon-based composite, with and without adsorbates, was determined by potentiometric titration. The  $\sigma_0$  values as a function of the solution pH were calculated using the computer program "titr\_v3", on the basis of the difference in the volume of the titrant added to the suspension and the supporting electrolyte solution providing a specific pH value [30]. The titration was

performed using a set that consisted of: teflon vessel connected to a RE 204 thermostat (Lauda, Lauda-Königshofen, Germany), automated Dosimat 765 microburette (Metrohm, Herisau, Switzerland), glass and calomel electrodes (Beckman Instruments, Pasadena, CA, USA), PHM 240 pH meter (Radiometer, Copenhagen, Denmark) and a computer. The examined samples were titrated with 0.1 M NaCl solution, in the pH range from 3 to 11. The solutions were prepared by adding 0.03 g Na-X or 0.075 g Na-X(C) to 50 cm<sup>3</sup> of supporting electrolyte (0.001 M NaCl). At first, only the electrolyte was titrated, then the suspensions, with and without adsorbates (10 ppm), was examined.

The measurements of the electrophoretic mobility ( $u_e$ ) enabled the calculation of the zeta potential ( $\zeta$ ) of the particles of zeolite and its carbon composite [31]. The experiments were carried out using the Zetameter Nano ZS (Malvern Instruments, Cambridge, UK). The suspensions were prepared by adding 0.01 g of Na-X or Na-X(C) to 200 cm<sup>3</sup> of the supporting electrolyte solution (0.001 M NaCl), with and without one or two heavy metal ions (10 ppm). After a 3-min sonication, the suspension was divided into several parts and a specific pH value was adjusted in each of them (in the range from 3 to 10).

### 3. Results and Discussion

#### 3.1. Physicochemical Properties of Adsorbents

The textural parameters of zeolite and zeolite–carbon composite are summarized in Table 1.

**Table 1.** Textural parameters of Na-X and Na-X(C) materials:  $S_{BET}$ —specific surface area,  $S_{micro}$ —micropore area,  $V_t$ —total pore volume,  $V_{micro}$ —micropore volume,  $D$ —average pore diameter.

Material	$S_{BET}$ (m <sup>2</sup> /g)	$S_{micro}$ (m <sup>2</sup> /g)	$V_t$ (cm <sup>3</sup> /g)	$V_{micro}$ (cm <sup>3</sup> /g)	$D$ (4V/A) (nm)
Na-X	728	694	0.31	0.27	1.73
Na-X(C)	272	189	0.17	0.07	2.56

The obtained textural parameters indicated that zeolite Na-X was characterized by a more developed surface than its carbon composite. Na-X has a much higher specific surface area (728 m<sup>2</sup>/g) and greater content of micropores in its structure (about 87%). In the case of the Na-X(C) composite, the results are in agreement with those obtained by other authors [19]. For Na-X, the  $S_{BET}$  value is even higher than for commercial 13X or those obtained from chemical reagents [32]. It should be mentioned that when zeolite was obtained directly from waste, e.g., from fly ash, the  $S_{BET}$  value is much lower ranged from 236 to 257 m<sup>2</sup>/g [33,34].

The chemical composition of zeolite–carbon Na-X(C) composite and Na-X zeolite is presented in Table 2.

**Table 2.** Elemental composition of Na-X(C) and Na-X adsorbents (%).

Adsorbent	Compounds											
	Na <sub>2</sub> O	MgO	Al <sub>2</sub> O <sub>3</sub>	SiO <sub>2</sub>	P <sub>2</sub> O <sub>5</sub>	SO <sub>3</sub>	K <sub>2</sub> O	CaO	TiO <sub>2</sub>	Fe <sub>2</sub> O <sub>3</sub>	LOI	C
Na-X	7.32	1.69	23.41	41.12	0.02	-	0.71	7.48	0.05	1.31	16.88	-
Na-X(C)	3.53	1.21	14.37	28.19	0.05	0.48	1.34	2.21	1.05	9.33	38.23	31.46

The chemical composition of the Na-X(C) composite and Na-X zeolite is dominated by silicon 28.19% and 41.12% and aluminum by 14.37% and 23.41%, respectively. Moreover, there are negligible amounts of CaO (2.21–7.48%), Fe<sub>2</sub>O<sub>3</sub> (1.31–9.33%) and Na<sub>2</sub>O (3.53–7.32%). It is worth mentioning that Si/Al molar ratios for Na-X and Na-X(C) was 1.49 and 1.66, respectively. It can be found that Na-X(C) has high Si/Al molar ratio. The Si/Al molar ratio values highly correspond to the results obtained by other researchers [18,19]. Boycheva, with coworkers, determined a similar Si/Al molar ratio (1.37–1.60) for Na-X





case, a chemical analysis showed the presence of C, and in the second case, the dominant elements were Al, Si, Na, Mg and O. The C presence in the sample was dictated by the sample preparation. Figure 3 shows the morphology of pure Na-X zeolite (no ash residue).

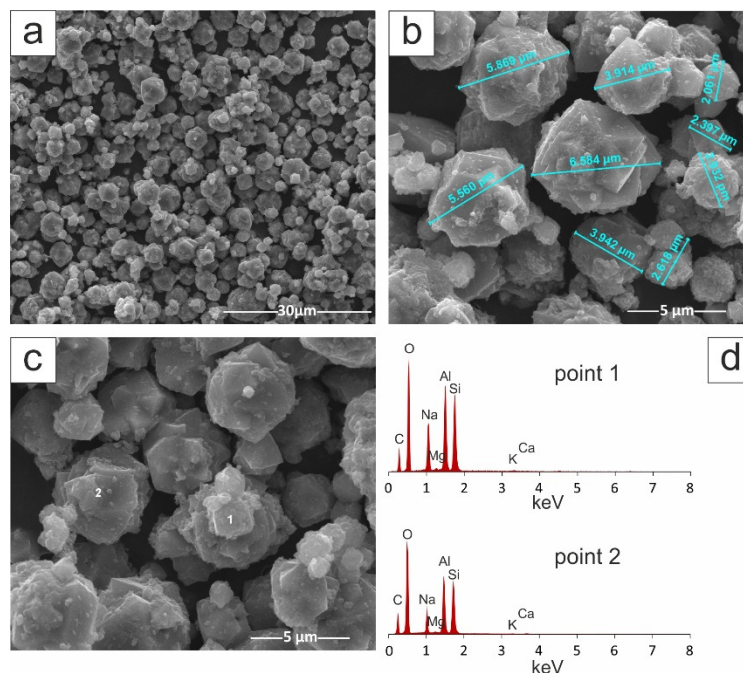


**Figure 3.** SEM images of Na-X sample: (a) 4000× magnification, (b) 16,000× magnification, (c) 16,000× magnification with EDS chemical analysis (d).

The zeolite crystals are very well formed with a size from 2 μm to 5 μm. Figure 3 also shows the EDS analysis performed on zeolite crystals (points 1 and 2). In both cases, the dominant elements were Si, Al, Na and O and small amounts of Ca, K and Mg. The presence of C in the sample was associated with the sample preparation.

Diffractograms of the phase composition of Na-X(C) composite and pure Na-X zeolite are shown in Figure 4.

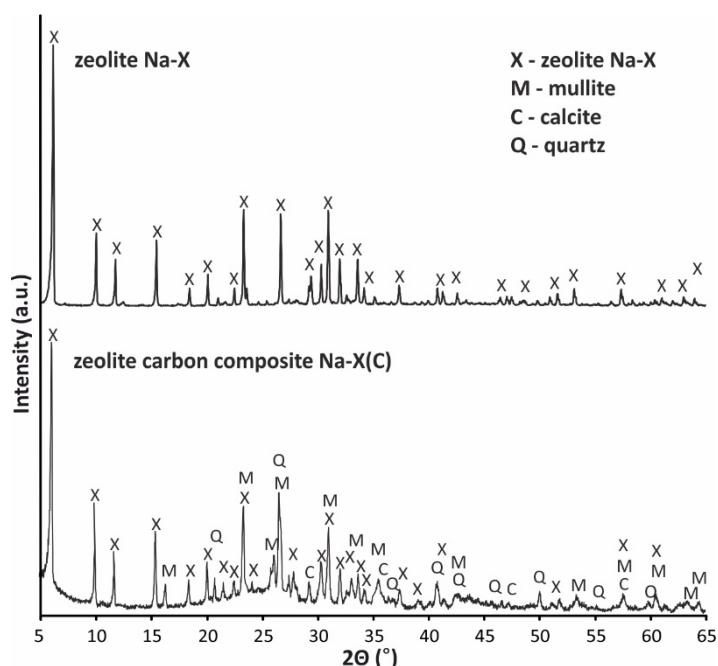


**Figure 4.** Phase analysis of zeolite–carbon Na-X(C) composite and Na-X zeolite.

The diffractograms of the Na-X(C) composite and Na-X zeolite indicate that only the pure Na-X zeolite sample obtained from the filtrate has a monomineral character. The presence of the zeolite phase was characterized by the following reflections  $d_{hkl} = 14.42; 8.83; 5.71; 3.83; 3.35; 2.90 \text{ \AA}$  (reference code 00-038-0237). In addition, on the diffractograms, a higher background level (between  $15$  and  $35^\circ 2\theta$ ) was not observed, which is normal for zeolites obtained directly from fly ash being a proof of amorphous aluminosilicate glaze presence [36]. On the other hand, on the diffractogram of composite phases related to unreacted ash residue in the form of aluminosilicate glaze, mullite ( $d_{hkl} = 5.38; 3.40; 2.79; 2.59 \text{ \AA}$ ; reference code 01-089-2645), quartz ( $d_{hkl} = 4.25; 3.34; 2.45; 2.28 \text{ \AA}$ ; reference code 01-073-8320) and calcite ( $d_{hkl} = 3.03; 2.49; 2.09; 1.88 \text{ \AA}$ ; reference code 01-086-2334) were observed. Such phase characteristics is typical for fly ash-derived zeolites [37].

The FTIR spectra of zeolite and zeolite–carbon composite are presented in Figure 5.

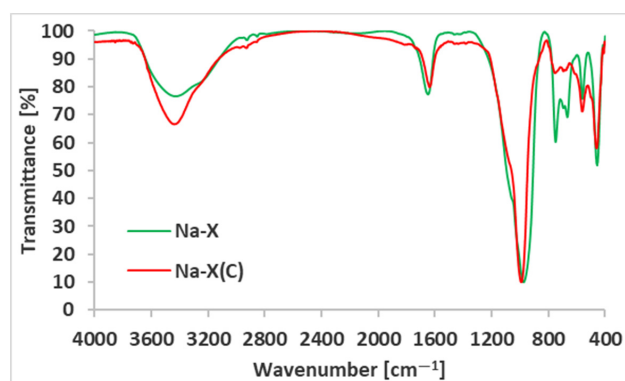


Figure 5. FTIR spectra of Na-X and Na-X(C).

The FTIR spectra of zeolite and zeolite–carbon composite contained the following bands at:  $3386.39 \text{ cm}^{-1}$  and  $1636.30 \text{ cm}^{-1}$  (corresponding with stretching and bending of water molecules adsorbed on solids),  $979.66 \text{ cm}^{-1}$  (Si-O-Al anti-symmetric stretching vibration of T-O bonds, T—tetrahedrally bonded Si or Al),  $550.09 \text{ cm}^{-1}$  (symmetric stretching of double six membered rings of T-O-T),  $449.33 \text{ cm}^{-1}$  (symmetric T-O bending). The spectrum of pure zeolite contained two additional bands at:  $741.97 \text{ cm}^{-1}$  and  $658.57 \text{ cm}^{-1}$ , which can be attributed to symmetric T-O-T stretching and symmetric Si-O-Si stretching, respectively. All above bands are typical for zeolites X [38].

### 3.2. $\text{Zn}^{2+}$ and $\text{Pb}^{2+}$ Adsorption on Zeolite and Zeolite–Carbon Composite in the Single Systems

Figure 6a,b present the measured adsorbed amounts of heavy metal ions on zeolite and zeolite–carbon composite over time.

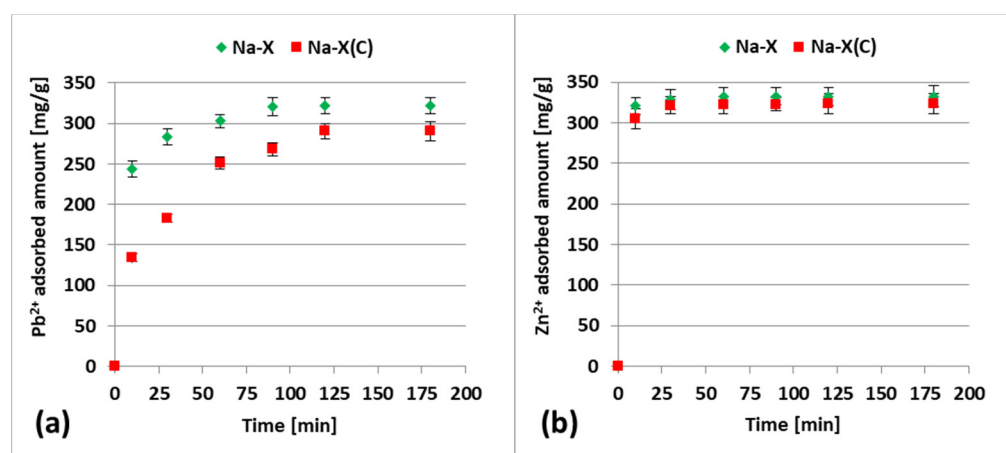


Figure 6. Adsorption kinetics of  $\text{Pb}^{2+}$  (a) and  $\text{Zn}^{2+}$  (b) on the Na-X and Na-X(C) surface in the single systems, at pH 5.



Experimental data were fitted to the commonly applied kinetic models—the pseudo-first-order and pseudo-second-order equations. The calculated parameters indicated the best fitting of experimental data to the pseudo-second-order model. The  $R^2$  values were as follows: 0.999 (Na-X +  $Pb^{2+}$ ), 0.997 (Na-X(C) +  $Pb^{2+}$ ), 1.000 (Na-X +  $Zn^{2+}$ ) and Na-X(C) +  $Zn^{2+}$ ; Table 3).

**Table 3.** Kinetics parameters of  $Pb^{2+}$  and  $Zn^{2+}$  adsorption on Na-X and Na-X(C) at pH 5.

Pseudo-II-Order Model					
System		$q_e$ (mg/g)	$k_2$ (g/(mg·min))	$R^2$	Linear Form
$Pb^{2+}$	Na-X	333.333	0.0007	0.999	$y = 0.003x + 0.0129$
	Na-X(C)	322.581	0.0002	0.997	$y = 0.0031x + 0.0533$
$Zn^{2+}$	Na-X	333.333	0.0090	1.000	$y = 0.003x + 0.001$
	Na-X(C)	322.581	0.0069	1.000	$y = 0.0031x + 0.0014$

According to the literature [39,40], a good fitting of experimental data to the PSO model indicated that the adsorption process was based on chemical interactions (chemisorption). The valence forces through the exchange or sharing of electrons between adsorbate and adsorbent. Such a good fitting of experimental data to PSO was also observed during the study on lead(II), chromium(VI) and copper(II) adsorption on kaolinite [41–43], as well as copper(II) and silver(I) ions on biochar [44,45]. However, it must be emphasized that some researchers do not agree with these assumptions. Płaziński and Rudziński [46] stated that the PSO/PFO models are not able to reflect changes in the mechanism controlling the adsorption kinetics. Thus, these equations do not represent any specific physical model. Qiu et al. [47] wrote that in many cases kinetic models are applied in an unsuitable or improper manner due to their boundary conditions.

The obtained results showed that in the single systems (containing only one heavy metal) the equilibrium state was reached faster for  $Zn^{2+}$  ions than for  $Pb^{2+}$ —120 min for  $Pb^{2+}$  and 10 min for  $Zn^{2+}$ . After these times, the amount of the ions adsorbed on the solid surface does not change over time. The calculated  $k_2$  values for  $Zn^{2+}$  adsorption was significantly higher (compared to  $Pb^{2+}$ ) and were in the range 0.0069–0.0090 g/mg·min.

Figure 7a,b show the experimental adsorption isotherms for  $Zn^{2+}$  and  $Pb^{2+}$  ions on the Na-X and Na-X(C) surfaces in the single systems.

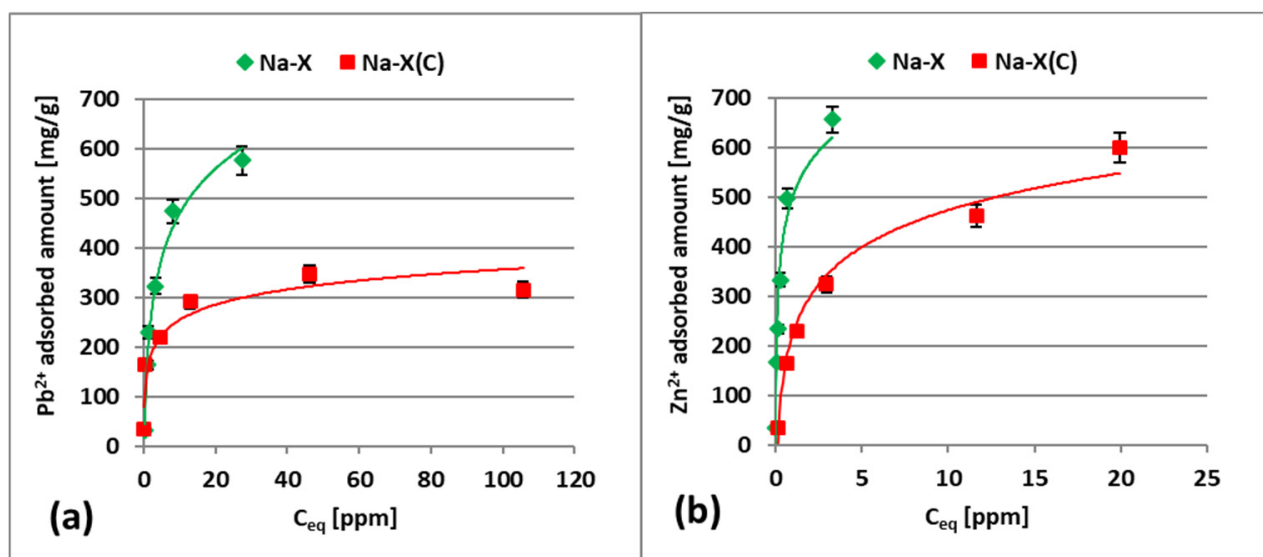


**Figure 7.** Adsorption isotherms of  $Pb^{2+}$  (a) and  $Zn^{2+}$  ions (b) on the Na-X and Na-X(C) surfaces in the single systems at pH 5.

The isotherm parameters calculated using Langmuir and Freundlich models are shown in Table 4.

**Table 4.** Isotherm parameters of  $Pb^{2+}$  and  $Zn^{2+}$  adsorption on the Na-X and Na-X(C) surfaces at pH 5.

System		Langmuir Model			Freundlich Model		
		$q_m$ (mg/g)	$K_L$ ( $dm^3/mg$ )	$R^2$	$n$	$K_F$ ( $mg/g (mg/dm^3)^{-1/nF}$ )	$R^2$
$Pb^{2+}$	Na-X	676.594	0.227	0.966	1.625	0.0005	0.794
	Na-X(C)	321.909	1.178	0.997	2.501	0.0014	0.719
$Zn^{2+}$	Na-X	693.289	4.878	0.997	2.148	0.0002	0.943
	Na-X(C)	640.938	0.395	0.979	1.899	0.0006	0.916

The experimental data were better fitted to the Langmuir model. The  $R^2$  values for all systems were very high and equal to 0.966 (Na-X +  $Pb^{2+}$ ), 0.997 (Na-X(C) +  $Pb^{2+}$  and Na-X +  $Zn^{2+}$ ) and 0.979 (Na-X(C) +  $Zn^{2+}$ ). Therefore, it can be assumed that  $Pb^{2+}$  and  $Zn^{2+}$  form monolayers on the Na-X and Na-X(C) surfaces and all adsorption sites are energetically equivalent [27,40,48]. A good fitting of experimental data to the Langmuir model was also observed for the systems: kaolinite- $Pb^{2+}$ , kaolinite-Cr(VI), kaolinite- $Cu^{2+}$  and activated biochar- $Cu^{2+}$  [41–43,45]. The obtained data also indicated that larger amounts of metal ions were adsorbed on the zeolite than on its carbon composite. The  $q_m$  parameter (indicating maximum adsorption capacity in Langmuir model) of zeolite relative to  $Pb^{2+}$  ions equal 676.59 mg/g, whereas zeolite relative to  $Zn^{2+}$  ions equal 321.91 mg/g. On the other hand, the  $q_m$  value of zeolite–carbon composite was 693.29 mg/g and 640.94 mg/g relative to  $Pb^{2+}$  and  $Zn^{2+}$ , respectively. The higher adsorption capacity of zeolite (compared to zeolite–carbon composite) is mainly dictated by its larger specific surface area. The  $S_{BET}$  parameter of Na-X is 456  $m^2/g$  higher than that of Na-X(C). Moreover, pure zeolite is characterized by higher volume of micropores ( $V_{micro}$  is equal to 0.27  $cm^3/g$  and 0.07  $cm^3/g$  for Na-X and Na-X(C), respectively).

The adsorbed amounts of  $Zn^{2+}$  observed for both adsorbents were significantly higher than those of  $Pb^{2+}$ . It can be explained by differences in the ion sizes—zinc has a much smaller ionic radius (0.74 Å) than lead (1.29 Å) [49,50]. Owing to the smaller size,  $Zn^{2+}$  ions reach active sites of adsorbent faster. During the adsorption, cations located in zeolite pores can be replaced with heavy metal ions. This ion exchange is easier for  $Zn^{2+}$  ions and occurs according to equation (Equation (5)) [50]:



The point of zero charge ( $pH_{pzc}$ ) of zeolite is about 9, whereas of Na-X(C) is 8.5. At pH values lower than  $pH_{pzc}$ , the adsorbent surface has a positive charge, whereas at pH values higher than  $pH_{pzc}$  the adsorbent surface assumes a negative charge. Thus at pH 5, when both adsorbent and adsorbate have a charge of the same sign, there is an electrostatic repulsion between the system compounds. However, despite the presence of these forces, heavy metal ions can be adsorb from the solution efficiently. This is probably dictated by the large specific surface area of the solids and their unique structure composed of three-dimensional channels and pore system allowing exchange of ions [1,2].

### 3.3. $Zn^{2+}$ and $Pb^{2+}$ Adsorption on Zeolite and its Composite in the Mixed Systems

Figure 8a,b present adsorption kinetics of  $Zn^{2+}$  and  $Pb^{2+}$  on Na-X and Na-X(C) in the mixed systems (i.e., containing both heavy metals at the same time). In turn, Figure 9 summarizes the adsorbed amounts of heavy metals on both adsorbents noted in the single and mixed systems.

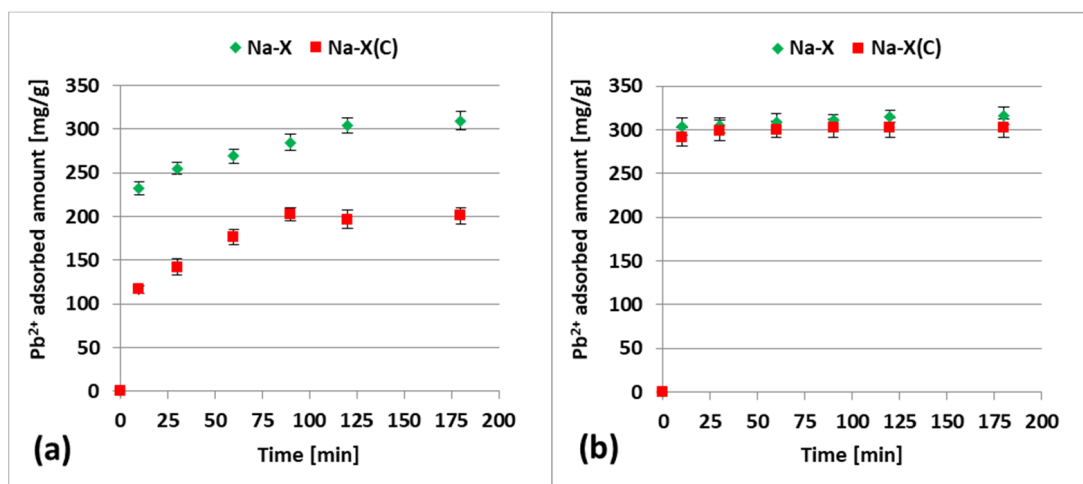


Figure 8. Adsorption kinetics of  $Pb^{2+}$  (a) and  $Zn^{2+}$  (b) on Na-X and Na-X(C) in the mixed systems, at pH 5.

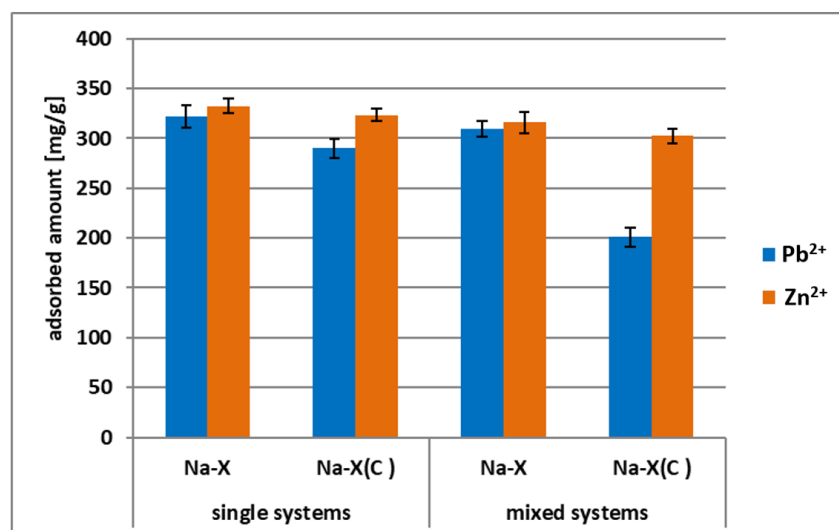
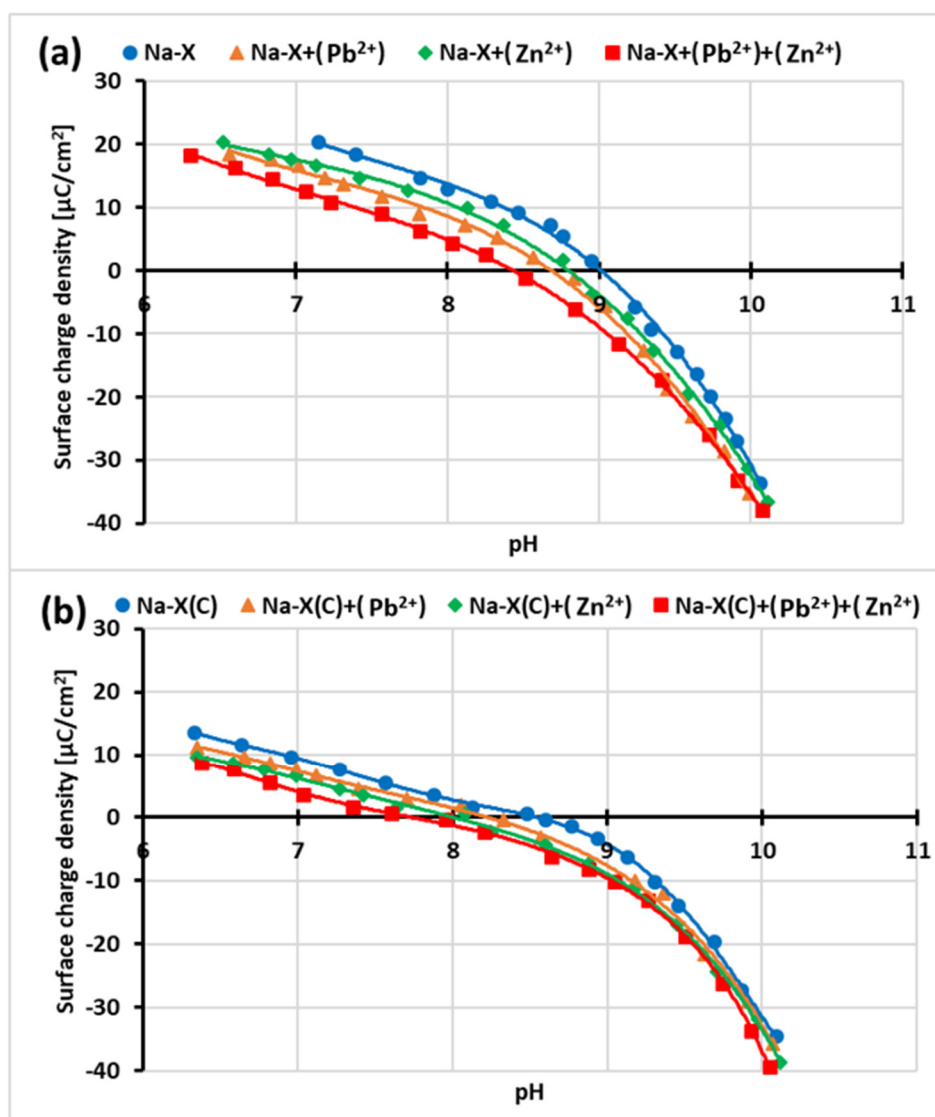


Figure 9. Comparison of adsorbed amounts of  $Pb^{2+}$  and  $Zn^{2+}$  on Na-X and Na-X(C) in the mixed systems, in an equilibrium state at pH 5.

The obtained data indicated that the adsorbed amounts observed in the mixed systems were clearly lower than those noted in the single ones. The differences were noticeable for both heavy metal ions. In case of  $Pb^{2+}$  ions, the adsorbed amount on the Na-X surface decreased from 322.1 mg/g to 309.36 mg/g, whereas on the Na-X(C) surface, it decreased from 290.11 mg/g to 200.76 mg/g. In the case of  $Zn^{2+}$  ions, the adsorbed amount on the Na-X surface decreased from 332.506 mg/g to 315.74 mg/g, in turn on the Na-X(C) surface it decreased from 323.53 mg/g to 302.56 mg/g. Thus, there is a competition between  $Zn^{2+}$  and  $Pb^{2+}$  ions for the adsorbent active sites in the mixed systems. However, it must be emphasized that the simultaneous addition of two ions to the system did not significantly affect the time needed to reach equilibrium. These times, noted in the mixed solutions, were identical to those observed in the single ones and equaled 120 min for  $Pb^{2+}$  ions and 10 min for  $Zn^{2+}$  ions.

### 3.4. Impact of $Zn^{2+}/Pb^{2+}$ Adsorption on Surface Charge Density of Na-X and Na-X(C) Particles

Figure 10a,b present changes in the surface charge density ( $\sigma_0$ ) of Na-X and Na-X(C) materials as a function of the solution pH.

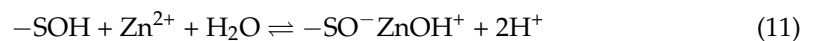
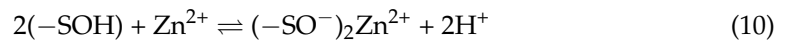
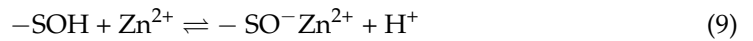
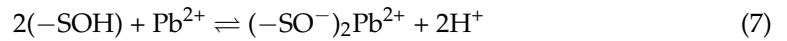
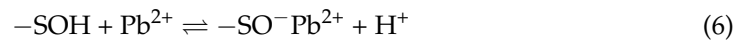


**Figure 10.** Surface charge density vs. solution pH of Na-X (a) and Na-X(C) (b) with and without one or two heavy metal ions.

The obtained titration curves indicated that at pH 5, at which the adsorption measurements were performed, both Na-X and Na-X(C) have a positively charged surface. Thus the repulsion between surface groups and heavy metal occurs at pH 5. Despite these unfavorable electrostatic conditions, adsorption of Pb<sup>2+</sup> and Zn<sup>2+</sup> takes place through chemical interactions (which was discussed above). The point of zero charge (pH<sub>pzc</sub>) for Na-X is about 9, whereas for Na-X(C) it is 8.5. The pH<sub>pzc</sub> falls at pH value for which the concentrations of the positively and negatively charged surface groups are the same (i.e.,  $\sigma_0 = 0$ ). For both adsorbents, the addition of heavy metal ions causes a decrease in pH<sub>pzc</sub> values. The pH<sub>pzc</sub> changes of Na-X particles are noticeable when Zn<sup>2+</sup> and Pb<sup>2+</sup> are added—their values decrease to about 8.8 and 8.6, respectively. The addition of both ions simultaneously causes further decrease of pH<sub>pzc</sub> to 8.5. When Pb<sup>2+</sup> and Zn<sup>2+</sup> are added to the system separately containing Na-X(C), a decrease in pH<sub>pzc</sub> values to 8.3 and 8.1 was observed. In turn, the addition of both ions lowers the pH<sub>pzc</sub> to 7.8.

The addition of divalent cations caused a decrease in the pH<sub>pzc</sub> value of both the zeolite and its composite with carbon (Equations (6–11)). It is related to the decrease in the value of the surface charge density due to the formation of an additional number of

negatively charged groups on the adsorbent surface. This phenomenon results from the interaction of metal cations with the solid surface groups, according to the equations [51,52]:



Simple ion adsorption affects usually the surface charge of adsorbents. It was described, inter alia, by Fijałkowska et al. [41,53–55]. In their studies,  $\text{Pb}^{2+}$  ions caused an increase in the negative values of  $\sigma_0$  of two clay minerals, kaolinite and montmorillonite. A similar behavior was observed for the  $\text{Cu}^{2+}$  ions adsorption on the carbon–silica composite surface [56,57].

### 3.5. Impact of $\text{Zn}^{2+}/\text{Pb}^{2+}$ Adsorption on Zeta Potential of Na-X and Na-X(C) Particles

Figure 11a,b present the pH effect on the zeta potential of adsorbent particles.

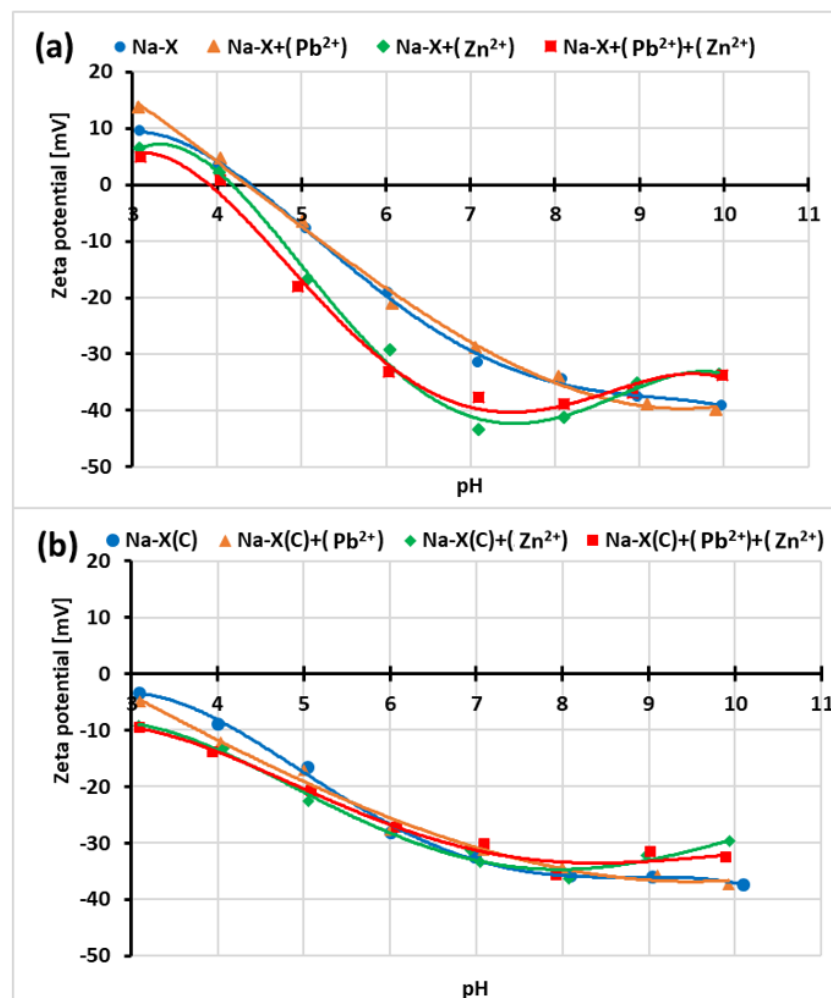


**Figure 11.** Zeta potential vs. solution pH of Na-X (a) and Na-X(C) (b) particles with and without one or two heavy metal ions.



The isoelectric point ( $\text{pH}_{\text{iep}}$ ) of the zeolite particles occurs at about pH 4.5. In the case of Na-X(C) particles,  $\text{pH}_{\text{iep}}$  is not observed in the studied pH range. The iep is at pH value for which the concentrations of the positively and negatively charged ions in the slipping plane area are the same (i.e.,  $\zeta = 0$ ). At a pH below  $\text{pH}_{\text{iep}}$ , the zeta potential becomes positive due to the predominance of positively charged ions in the slipping plane area. On the other hand, at pH below  $\text{pH}_{\text{iep}}$ , this trend is opposite (negatively charged ions dominate in the slipping plane area). Moreover, the iep value for zeolite materials without adsorbates are significantly different from the pzc values. This is mainly due to the overlapping of the diffusion parts of the electrical double layer formed on the opposite walls inside the relatively small solid pores. Such behavior was also observed for suspensions containing other zeolites [58–60].

The changes in the  $\text{pH}_{\text{iep}}$  of Na-X particles are noticeable when  $\text{Zn}^{2+}$  and both cations are added, the  $\text{pH}_{\text{iep}}$  values decrease to about 4.1 and 3.9, respectively. The addition of  $\text{Pb}^{2+}$  does not significantly affect this parameter. In the case of Na-X(C), the addition of ions practically does not change the zeta potential of solid particles. At pHs equal or higher than 8.5, there is a trend of decrease in the zeta potential with pH increase. It is observed especially in single systems containing  $\text{Zn}^{2+}$  ions. This is due to overcharging or overloading of the electrical double layer, i.e., charge reversal. This phenomenon is related to the occurrence of more numerous ions on the inner part of the electrical double layer than the ions on the solid surface. Consequently, the same charge sign appears on the outside part of the electrical double layer and also on the surface [61].

The zeta potential decides the stability of solid particles covered with adsorption layers. This parameter is very important for the effective separation of the solid with adsorbed heavy metals from the liquid phase. In the examined system, zeta potential values in all examined systems at pH 5 (at which adsorption of heavy metals was performed) changes from  $-5$  to  $-22$  mV. Such values of electrokinetic potential do not guarantee effective suspensions stabilization. According to the literature [62], the colloidal system is stable when absolute values of zeta potential of the particles exceed 30 mV.

### 3.6. Desorption of $\text{Zn}^{2+}$ and $\text{Pb}^{2+}$ from Zeolite and Its Composite

The desorption degrees observed for the solids are shown in Table 5.

**Table 5.** Desorption degree (%) of  $\text{Zn}^{2+}$  and  $\text{Pb}^{2+}$  ions from the Na-X and Na-X(C) surface in single and mixed systems, obtained using 0.1 M HCl or 0.1 M NaOH.

Desorbing Agent	Desorbed Ion	Na-X	Na-X(C)
		Single Systems	
HCl	$\text{Pb}^{2+}$	$61.00 \pm 1.5$	$39.55 \pm 1.6$
NaOH		$17.13 \pm 0.6$	$12.29 \pm 0.4$
HCl	$\text{Zn}^{2+}$	$6.11 \pm 0.1$	$3.82 \pm 0.2$
NaOH		$2.48 \pm 0.1$	$1.32 \pm 0.1$
<b>Mixed Systems</b>			
HCl	$\text{Pb}^{2+}$	$77.94 \pm 2.1$	$64.31 \pm 1.8$
NaOH		$24.82 \pm 1.2$	$22.33 \pm 1.5$
HCl	$\text{Zn}^{2+}$	$6.43 \pm 0.2$	$4.08 \pm 0.1$
NaOH		$2.61 \pm 0.1$	$1.41 \pm 0.1$

These results indicated significantly larger desorption using 0.1 M HCl than 0.1 M NaOH. Furthermore, the measured desorbed amounts were higher for  $\text{Pb}^{2+}$  ions than  $\text{Zn}^{2+}$  ones. These trends were observed for both Na-X and Na-X(C), in the single and mixed systems.

The higher desorption of  $\text{Pb}^{2+}$  ions is caused by the fact that during the adsorption  $\text{Zn}^{2+}$  cations are exchanged more effectively with the ions located in the structure of zeolite

or zeolite–carbon composite.  $\text{Pb}^{2+}$  ions, owing to their larger size, do not penetrate the pores and channels in such a great degree as  $\text{Zn}^{2+}$  ones, so their desorption is easier.

#### 4. Conclusions

In this work, Na-X zeolites and a carbon zeolite composite Na-X(C) were used to remove  $\text{Zn}^{2+}$  and  $\text{Pb}^{2+}$  (single and mixed systems) from aqueous solutions. Pure zeolite was characterized by a more developed surface than zeolite–carbon composite. The adsorption of  $\text{Zn}^{2+}$  ions occurs very quickly and efficiently, which is evidenced by the achievement of equilibrium in both systems ( $\text{Zn}^{2+}$  + Na-X/Na-X(C)) just after 10 min. Due to the larger specific surface area of Na-X, the ion adsorption is more efficient on its particles than on the Na-X(C) ones. Experimental data of adsorption kinetics were the best fitted to the pseudo-second-order model. In turn, the obtained adsorption isotherms were better fitted to the Langmuir model. In the mixed systems, there is a competition between the heavy metal ions, which leads to reduced adsorption of  $\text{Pb}^{2+}$  and  $\text{Zn}^{2+}$ . The addition of divalent cations decreases the  $\text{pH}_{\text{pzc}}$  of the studied systems due to the induction of additive negative sites on the adsorbent surface. More efficient desorption of heavy metals from the solids was achieved using hydrochloric acid. Less efficient desorption of  $\text{Zn}^{2+}$  ions indicates a stronger binding of this ion to the surface of adsorbents. The novelty of the research is the fact that a new way to dispose of fly ash has been successfully discovered. A normal use of such waste (e.g., in construction industry), is not possible due to the high carbon content. Using the secondary waste (silica and alumina rich solution) for the production of pure zeolite (Na-X) is another innovative aspect of this study. These facts, combined with the possibility of producing adsorbents on a semi-technical scale, will allow to reduce the amount of disposed fly ash, and contribute to more efficient heavy metals removal from aqueous solutions.

**Author Contributions:** Conceptualization, R.P., M.W.; methodology, R.P., M.W., K.S.-K., K.J.; software, R.P., K.S.-K.; validation, R.P., M.W.; formal analysis, M.W., R.P., M.F.; investigation, R.P., M.M., M.W., K.S.-K., K.J., M.F.; resources, R.P., M.F.; data curation, M.M., M.W., R.P., K.S.-K.; writing—original draft preparation, R.P., M.M., K.S.-K.; writing—review and editing, M.W., K.S.-K.; visualization, M.M., R.P., M.W., K.S.-K., M.F.; supervision, M.W.; project administration, R.P.; funding acquisition, R.P., M.F. All authors have read and agreed to the published version of the manuscript.

**Funding:** This work was financed by the National Centre for Research and Development project Lider contract number LIDER/19/0072/L-9/17/NCBR/2018.

**Institutional Review Board Statement:** Not applicable.

**Informed Consent Statement:** Not applicable.

**Data Availability Statement:** The data presented in this study are available on request from the corresponding author.

**Acknowledgments:** We would like to thank Wojciech Franus for his scientific support.

**Conflicts of Interest:** The authors declare no conflict of interest.

#### References

1. Gottardi, G.; Galli, E. *Natural Zeolites*; Springer: Berlin/Heidelberg, Germany, 1985; pp. 1–34.
2. Pleśniak, J.; Trzop, W. Everyday life with zeolite. *Analit* **2016**, *2*, 146–151. (In Polish)
3. Szala, B.; Turek, P.; Jeleń, A.; Bajda, T. Synthesis and sorption properties of organo-zeolites. *ZN UZ IŚ* **2013**, *30*, 5–12. (In Polish)
4. Biegańska, M. Use of the Bark of the Braided Willow *Salix americana* for Adsorption of Heavy Metals. Ph.D. Thesis, Poznań University of Economics and Business, Poznań, Poland, 2011; pp. 64–66. (In Polish).
5. Inglezakis, V.J.; Zorpas, A.A. *Handbook of Natural Zeolites*; Bentham Science: Sharjah, United Arab Emirates, 2012; pp. 3–133.
6. Muir, B. Production and Utilization of Organo-Zeolites as Petroleum Sorbents. Ph.D. Thesis, AGH University of Science and Technology, Kraków, Poland, 2016; pp. 12–32. (In Polish).
7. Shahrokhi-Shahraki, R.; Benally, C.; El-Din, M.G.; Park, J. High efficiency removal of heavy metals using tire derived activated carbon vs. commercial activated carbon: Insights into the adsorption mechanisms. *Chemosphere* **2021**, *264*, 128455. [[CrossRef](#)]
8. Kobayashi, Y.; Ogata, F.; Nakamura, T.; Kawasaki, N. Synthesis of novel zeolites produced from fly ash by hydrothermal treatment in alkaline solution and its evaluation as an adsorbent for heavy metal removal. *J. Environ. Chem. Eng.* **2020**, *8*, 103687. [[CrossRef](#)]

9. Visa, M. Synthesis and characterization of new zeolite materials obtained from fly ash for heavy metals removal in advanced wastewater treatment. *Powder Technol.* **2016**, *294*, 338. [[CrossRef](#)]
10. Cheng, T.; Chen, C.; Tang, R.; Han, C.H.; Tian, Y. Competitive adsorption of Cu, Ni, Pb, and Cd from aqueous solution onto fly ash-based linde F(K) Zeolite. *Iran. J. Chem. Chem. Eng.* **2018**, *37*, 61.
11. Joseph, I.V.; Tosheva, L.; Doyle, A.M. Simultaneous removal of Cd(II), Co(II), Cu(II), Pb(II), and Zn(II) ions from aqueous solutions via adsorption on FAU-type zeolites prepared from coal fly ash. *J. Environ. Chem. Eng.* **2020**, *8*, 103895. [[CrossRef](#)]
12. Kragović, M.; Pašalić, S.; Marković, M.; Petrović, M.; Nedeljković, B.; Momčilović, M.; Stojmenović, M. Natural and Modified Zeolite—Alginate Composites. Application for Removal of Heavy Metal Cations from Contaminated Water Solutions. *Minerals* **2018**, *8*, 11. [[CrossRef](#)]
13. Kim, S.A.; Kamala-Kannan, S.; Lee, K.-J.; Park, Y.-J.; Shea, P.J.; Lee, W.-H.; Kim, H.-M.; Oh, B.-T. Removal of Pb(II) from aqueous solution by a zeolite–nanoscale zero-valent iron composite. *Chem. Eng. J.* **2013**, *217*, 54–60. [[CrossRef](#)]
14. Li, Z.; Wang, L.; Meng, J.; Liu, X.; Xu, J.; Wang, F.; Brookes, P. Zeolite-supported nanoscale zero-valent iron: New findings on simultaneous adsorption of Cd(II), Pb(II), and As(III) in aqueous solution and soil. *J. Hazard. Mater.* **2018**, *344*, 1–11. [[CrossRef](#)]
15. Wang, J.; Li, Y.; Lv, Z.; Xie, Y.; Shu, J.; Alsaedi, A.; Hayat, T.; Chen, C. Exploration of the adsorption performance and mechanism of zeolitic imidazolate framework-8@graphene oxide for Pb(II) and 1-naphthylamine from aqueous solution. *J. Colloid Interf. Sci.* **2019**, *542*, 410–420. [[CrossRef](#)]
16. Abdelrahman, E.A.; Abou El-Reash, Y.G.; Youssef, H.M.; Kotp, Y.H.; Hegazey, R.M. Utilization of rice husk and waste aluminum cans for the synthesis of some nanosized zeolite, zeolite/zeolite, and geopolymer/zeolite products for the efficient removal of Co(II), Cu(II), and Zn(II) ions from aqueous media. *J. Hazard. Mater.* **2020**, *401*, 123813. [[CrossRef](#)]
17. Wang, Z.; Tan, K.; Cai, J.; Hou, S.; Wang, Y.; Jiang, P.; Liang, M. Silica Oxide Encapsulated Natural Zeolite for High Efficiency Removal of Low Concentration Heavy Metals in Water. *Colloids Surf. A* **2019**, *561*, 388–394. [[CrossRef](#)]
18. Panek, R.; Madej, J.; Bandura, L.; Słowik, G. Recycling of Waste Solution after Hydrothermal Conversion of Fly Ash on a Semi-Technical Scale for Zeolite Synthesis. *Materials* **2021**, *14*, 1413. [[CrossRef](#)]
19. Bandura, L.; Panek, R.; Madej, J.; Franus, W. Synthesis of zeolite–carbon composites using high-carbon fly ash and their adsorption abilities towards petroleum substances. *Fuel* **2021**, *283*, 119173. [[CrossRef](#)]
20. Bandura, L.; Franus, M.; Panek, R.; Wozzuk, A.; Franus, W. Characteristics of zeolites and their application as adsorbents of petroleum substances. *Przem. Chem.* **2015**, *93–94*, 323–327. (In Polish)
21. Lu, C.A.; Zhang, J.F.; Jiang, H.M.; Yang, J.C.; Zhang, J.T.; Wang, J.Z.; Shan, H.X. Assessment of soil contamination with Cd, Pb and Zn and source identification in the area around the Huludao Zinc Plant. *J. Hazard. Mater.* **2010**, *182*, 743–748. [[CrossRef](#)]
22. Fajardo, C.; Costa, G.; Nande, M.; Botías, P.; García-Cantalejo, J.; Martín, M. Pb, Cd, and Zn soil contamination: Monitoring functional and structural impacts on the microbiome. *Appl. Soil Ecol.* **2019**, *135*, 56–64. [[CrossRef](#)]
23. Rengel, Z.; Graham, R.D. Importance of seed Zn content for wheat growth on Zn-deficient soil. I. Vegetative growth. *Plant Soil* **1995**, *173*, 259–266. [[CrossRef](#)]
24. Sing, K.S.W.; Everett, D.H.; Haul, R.A.W.; Moscou, L.; Pierotti, R.A.; Rouquerol, J.; Siemieniowska, T. Reporting Physisorption Data For Gas/Solid Systems with Special Reference to the Determination of Surface Area and Porosity. *Pure Appl. Chem.* **1985**, *57*, 603–619. [[CrossRef](#)]
25. Thommes, M.; Kaneko, K.; Neimark, A.V.; Olivier, J.P.; Rodriguez-Reinoso, F.; Jean Rouquerol, J.; Sing, K.S.W. Physisorption of gases, with special reference to the evaluation of surface area and pore size distribution (IUPAC Technical Report). *Pure Appl. Chem.* **2015**, *87*, 9–10. [[CrossRef](#)]
26. Ościk, J. *Adsorption*; UMCS: Lublin, Poland, 1969; pp. 91–124. (In Polish)
27. Foo, K.Y.; Hameed, B.H. Insights into the modeling of adsorption isotherm systems. *Chem. Eng. J.* **2010**, *156*, 2–10. [[CrossRef](#)]
28. Ho, Y.S.; McKay, G. Sorption of dye from aqueous solution by peat. *Chem. Eng. J.* **1998**, *70*, 115–124. [[CrossRef](#)]
29. Ho, Y.S.; McKay, G. Application of kinetics models to the sorption of copper(II) onto peat. *Adsorpt. Sci. Technol.* **2002**, *20*, 797–815. [[CrossRef](#)]
30. Janusz, W. Electrical double layer at the metal oxide–electrolyte interface. In *Interfacial Forces and Fields: Theory and Applications*; Marcel Dekker Inc.: New York, NY, USA, 1999; Volume 85, Chapter 4.
31. Oshima, H. A simple expansion for Henry’s function for the retardation effect in electrophoresis of spherical colloidal particles. *J. Colloid Interface Sci.* **1994**, *168*, 269–271. [[CrossRef](#)]
32. Ansari, M.; Aroujalian, A.; Raisi, A.; Dabir, B.; Fathizadeh, M. Preparation and Characterization of Nano-NaX Zeolite by Microwave Assisted Hydrothermal Method. *Adv. Powder Technol.* **2014**, *25*, 722–727. [[CrossRef](#)]
33. Bandura, L.; Franus, M.; Józefaciuk, G.; Franus, W. Synthetic Zeolites from Fly Ash as Effective Mineral Sorbents for Land-Based Petroleum Spills Cleanup. *Fuel* **2015**, *147*, 100–107. [[CrossRef](#)]
34. Muriithi, G.N.; Petrik, L.F.; Doucet, F.J. Synthesis, Characterisation and CO<sub>2</sub> Adsorption Potential of NaA and NaX Zeolites and Hydrotalcite Obtained from the Same Coal Fly Ash. *J. CO<sub>2</sub> Util.* **2020**, *36*, 220–230. [[CrossRef](#)]
35. Boycheva, S.; Marinov, I.; Miteva, S.; Zgureva, D. Conversion of coal fly ash into nanozeolite Na-X by applying ultrasound assisted hydrothermal and fusion-hydrothermal alkaline activation. *Sustain. Chem. Pharm.* **2020**, *15*, 100217. [[CrossRef](#)]
36. Babajide, O.; Musyoka, N.; Petrik, L.; Ameer, F. Novel Zeolite Na-X Synthesized from Fly Ash as a Heterogeneous Catalyst in Biodiesel Production. *Catal. Today* **2012**, *190*, 54–60. [[CrossRef](#)]

37. Kunecki, P.; Panek, R.; Wdowin, M.; Bień, T.; Franus, W. Influence of the Fly Ash Fraction after Grinding Process on the Hydrothermal Synthesis Efficiency of Na-A, Na-P1, Na-X and Sodalite Zeolite Types. *Int. J. Coal Sci. Technol.* **2021**, *8*, 291–311. [[CrossRef](#)]
38. Zinal Abidin, A.; Abu Bakar, N.H.H.; Ng, E.P.; Tan, W.L. Rapid degradation of methyl orange by Ag doped zeolite X in the presence of borohydrite. *J. Taibah Univ. Sci.* **2017**, *11*, 1070–1079. [[CrossRef](#)]
39. Ho, Y.S.; McKay, G. Pseudo-second-order model for sorption process. *Process Biochem.* **1999**, *34*, 451–465. [[CrossRef](#)]
40. Jovanovic, M.; Rajic, N.; Obradovic, B. Novel kinetic model of the removal of divalent heavy metal ions from aqueous solutions by natural clinoptilolite. *J. Hazard. Mater.* **2012**, *233–234*, 57–64. [[CrossRef](#)] [[PubMed](#)]
41. Fijałkowska, G.; Szewczuk-Karpisz, K.; Wiśniewska, M. Anionic polyacrylamide as a substance strengthening the Pb(II) immobilization on the kaolinite surface. *Int. J. Environ. Sci. Technol.* **2020**, *17*, 1101–1112. [[CrossRef](#)]
42. Szewczuk-Karpisz, K.; Fijałkowska, G.; Wiśniewska, M.; Wójcik, G. Chromium(VI) reduction and accumulation on the kaolinite surface in the presence of cationic soil flocculant. *J. Soil Sediment.* **2020**, *20*, 3688–3697. [[CrossRef](#)]
43. Szewczuk-Karpisz, K.; Tomczyk, A.; Komaniecka, I.; Choma, A.; Adamczuk, A.; Sofińska-Chmiel, W. Impact of Sinorhizobium meliloti exopolysaccharide on adsorption and aggregation in the copper(II) ions/supporting electrolyte/kaolinite system. *Materials* **2021**, *14*, 1950. [[CrossRef](#)]
44. Tomczyk, A.; Sokołowska, Z.; Boguta, P.; Szewczuk-Karpisz, K. Comparison of monovalent and divalent removal from aqueous solutions using agricultural waste biochars prepared at different temperatures—Experimental and model study. *Int. J. Mol. Sci.* **2020**, *21*, 5851. [[CrossRef](#)]
45. Szewczuk-Karpisz, K.; Nowicki, P.; Sokołowska, Z.; Pietrzak, R. Hay-based activated biochars obtained using two different heating methods as effective low-cost sorbents: Solid surface characteristics, adsorptive properties and aggregation in the mixed Cu(II)/PAM system. *Chemosphere* **2020**, *250*, 126312. [[CrossRef](#)]
46. Płaziński, W.; Rudziński, W. Adsorption kinetics at solid/solution interfaces. The meaning of the pseudo-first- and pseudo-second-order equations. *Wiadomości Chem.* **2011**, *65*, 1055–1067.
47. Qiu, H.; Pan, B.-C.; Zhang, Q.-J.; Zhang, W.-M.; Zhang, Q.-X. Critical review in adsorption kinetic models. *J. Zhejiang Univ. Sci.* **2009**, *10*, 716–724. [[CrossRef](#)]
48. Ho, Y. The kinetics of sorption of divalent metal ions onto sphagnum moss peat. *Water Res.* **2000**, *34*, 735–742. [[CrossRef](#)]
49. Breviglieri, S.T.; Cavalheiro, É.T.G.; Chierice, G.O. Correlation between ionic radius and thermal decomposition of Fe(II), Co(II), Ni(II), Cu(II) and Zn(II) diethanoldithiocarbamates. *Thermochim. Acta* **2000**, *356*, 79–84. [[CrossRef](#)]
50. Lee, J.K.W.; Williams, I.S.; Ellis, D.J. Pb, U and Th diffusion in natural zircon. *Nature* **1997**, *390*, 159–162. [[CrossRef](#)]
51. Nibou, D.; Mekatel, H.; Amokrane, S.; Barkat, M.; Trari, M. Adsorption of Zn<sup>2+</sup> ions onto NaA and Na-X zeolites: Kinetic, equilibrium and thermodynamic studies. *J. Hazard. Mater.* **2010**, *173*, 637–646. [[CrossRef](#)] [[PubMed](#)]
52. Wiśniewska, M.; Fijałkowska, G.; Szewczuk-Karpisz, K.; Teresa, U.; Nosal-Wiercińska, A.; Wójcik, G. Comparison of adsorption affinity of anionic and cationic polyacrylamides for montmorillonite surface in the presence of chromium(VI) ions. *Adsorption* **2019**, *25*, 41–50. [[CrossRef](#)]
53. Fijałkowska, G.; Szewczuk-Karpisz, K.; Wiśniewska, M. Chromium(VI) and lead(II) accumulation at the montmorillonite/aqueous solution interface in the presence of polyacrylamide containing quaternary amine groups. *J. Mol. Liq.* **2019**, *293*, 1–8. [[CrossRef](#)]
54. Fijałkowska, G.; Wiśniewska, M.; Szewczuk-Karpisz, K. The structure of electrical double layer formed on the kaolinite surface in the mixed system of cationic polyacrylamide and lead(II) ions. *Physicochem. Probl. Miner. Process.* **2019**, *55*, 1339–1349.
55. Fijałkowska, G.; Szewczuk-Karpisz, K.; Wiśniewska, M. Anionic polyacrylamide influence on the lead(II) ion accumulation in soil—the study on montmorillonite. *J. Environ. Health Sci. Eng.* **2020**, *18*, 599–607. [[CrossRef](#)] [[PubMed](#)]
56. Szewczuk-Karpisz, K.; Wiśniewska, M.; Medykowska, M.; Galaburda, M.V.; Bogatyrov, V.M.; Oranska, O.I.; Blachnio, M.; Oleszczuk, P. Simultaneous adsorption of Cu(II) ions and poly(acrylic acid) on the hybrid carbon-mineral nanocomposites with metallic elements. *J. Hazard. Mater.* **2021**, *412*, 125138. [[CrossRef](#)]
57. Szewczuk-Karpisz, K.; Wiśniewska, M.; Medykowska, M.; Bogatyrov, V.; Sokołowska, Z. Adsorption layer structure on the surface of carbon-silica composite in the presence of proteins of different internal stability and Cu(II) ions—the effect on solid aggregation. *J. Mol. Liq.* **2020**, *309*, 113072. [[CrossRef](#)]
58. Wiśniewska, M.; Fijałkowska, G.; Nosal-Wiercińska, A.; Franus, M.; Panek, R. Adsorption mechanism of poly(vinyl alcohol) on the surfaces of synthetic zeolites: Sodalite, Na-P1 and Na-A. *Adsorption* **2019**, *25*, 567–574. [[CrossRef](#)]
59. Wiśniewska, M.; Urban, T.; Chibowski, S.; Fijałkowska, G.; Medykowska, M.; Nosal-Wiercińska, A.; Franus, W.; Panek, R.; Szewczuk-Karpisz, K. Investigation of adsorption mechanism of phosphate(V) ions on the nanostructured Na-A zeolite surface modified with ionic polyacrylamide with regard to their removal from aqueous solution. *Appl. Nanosci.* **2020**, *10*, 4475–4485. [[CrossRef](#)]
60. Wiśniewska, M.; Franus, W.; Fijałkowska, G.; Ostolska, I.; Wójcik, G.; Nosal-Wiercińska, A.; Gościńska, J. Adsorption and electrokinetic studies of sodalite/lithium/poly(acrylic acid) aqueous system. *Physicochem. Probl. Miner. Process.* **2020**, *56*, 158–166. [[CrossRef](#)]
61. Lament, K. Study on the Mechanism of Adsorption of Ca<sup>2+</sup> and Fe<sup>2+</sup> Cations on Metal Oxides Using an Ion-Selective Electrode and a Combined Platinum Electrode. Ph.D. Thesis, Maria Curie-Skłodowska University, Lublin, Poland, 2021; pp. 97–102. (In Polish)
62. Riddick, T.M. *Control of Colloid Stability through Zeta Potentia*; Livingston Pub. Co. Edition: Wynnewood, PA, USA, 1968.